Contents lists available at ScienceDirect

Spectrochimica Acta Part A: Molecular and Biomolecular Spectroscopy

Synthesis, thermal and spectral characterization of nanosized $Ni_xMg_{1-x}Al_2O_4$ powders as new ceramic pigments via combustion route using 3-methylpyrozole-5-one as fuel

Ibrahim S. Ahmed *, Sayed A. Shama, Hassan A. Dessouki, Ayman A. Ali

Chemistry Department, Faculty of Science, Benha University, Benha City, Egypt

ARTICLE INFO

ABSTRACT

New $Ni_xMg_{1-x}Al_2O_4$ nanosized in different composition ($0.1 \le x \le 0.8$) powders have been synthesized successively for first time by using low temperature combustion reaction (LTCR) of corresponding metal chlorides, carbonates and nitrates as salts with 3-methylpyrozole-5-one (3MP5O) as fuel at 300 °C in open air furnace. Magnesium aluminate spinel ($MgAl_2O_4$) was used as crystalline host network for the synthesis of nickel-based nano ceramic pigments. The structure of prepared samples was characterized by using different techniques such as thermal analysis (TG–DTG/DTA), X-ray powder diffraction (XRD), Fourier transform infrared spectroscopy (FT-IR) and transmission electron microscopy (TEM). UV/Visible and Diffuse reflectance spectroscopy (DRS) using CIE-$L^*a^*b^*$ parameters methods have been used for color measurements. The obtained results reveal that $Ni_xMg_{1-x}Al_2O_4$ powder of samples is formed in the single crystalline and pure phase with average particle size of 6.35–33.11 nm in the temperature range 500–1200 °C. The density, particle size, shape and color are determined for all prepared samples with different calcination time and temperature.

1. Introduction

Nano pigments have recently gained a wide range of industrial applications [1,2]. The nano inorganic pigments are considered insoluble, chemically and physically inert into the substrate or binders, with a particle size less than 100 nm. For example, mica-based pigments (particle size less than 20 nm) with pearlescent effect are used in cosmetics, automobile coating and plastics [3–5]. Ceramic pigments based on oxides, spinels, aluminates, etc., are prepared with blends of oxides as starting mixtures with the proper particle size distribution of powders [6,7]. Spinel-type oxides AB_2O_4, where A and B stand for two different cations of comparable ionic sizes which are suitable for a wide range of applications, such as magnetic materials, refractory and semiconducting properties [8,9]. In recent years, much work has been done on the preparation and the optical properties of spinel materials [10–12]. Ceramic pigments are synthesized by several solution techniques such as sol–gel [13–16], co-precipitation [13], hydrothermal [14,15], alkoxides hydrolysis [16–18], Penchini method [19,20] and low combustion method [21–23]. The properties of final powder depend on the preparation methods and

calcination temperature and time. Modification of physical properties of solid solution can be associated with dopants cations and with changes defect in compounds structure. Nickel–iron black ceramic pigments [24] of $(Fe_{0.8}Mg_{0.2})(Fe_{0.2}Ni_{0.8}Cr)O_4$ prepared by polymeric gel routes, yellow pigments [25] of $Ti_{1-2x}Nb_xNi_xO_{2-x/2}$ synthesized using the sol–gel method, yellow or yellow-green pigments [26] cyclo-tetraphosphates of $Zn_{2-x}Ni_xP_4O_{12}$ as special pigment, yellow colored pigments [27] of $Zn_xNi_{1-x}WO_4$ obtained using a polymeric precursor method and the transition metal ions nickel-doped ZnO-based ceramic pale yellow pigments can be prepared by combustion synthesis [28–32]. The type of matrix, doping cation and its amount will show an effect on the pigment color.

In our previous work, we produce nanosized of ceramic pigments using urea as fuel [33,34]. The synthesis of homogeneous nanocrystalline powders of $Ni_xMg_{1-x}Al_2O_4$ structure as ceramic pigments via low temperature combustion method by using 3-methylpyrozole-5-one (3MP5O) as a fuel is prepared.

2. Experimental

2.1. Materials and reagents

All the starting chemicals used in this study are of pure grade: aluminum chloride hexahydrate ($AlCl_3 \cdot 6H_2O$) (Aldrich), magne-

* Corresponding author. Tel.: +20 0122408034; fax: +20 01333222875.
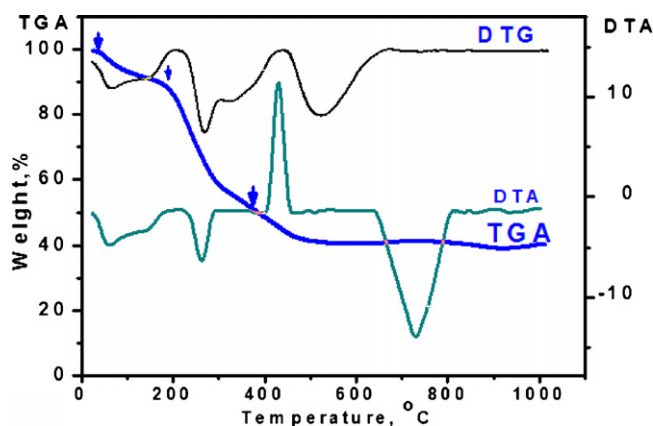 *E-mail address:* isahmed2010@gmail.com (I.S. Ahmed).

Fig. 1. Thermal analysis for 0.50 mol of Ni^{2+} system using 3-methyl pyrozole-5-one (3MP5O) as fuel.

sium chloride hexahydrate ($MgCl_2 \cdot 6H_2O$) (Aldrich), cobalt chloride hexahydrate ($NiCl_2 \cdot 6H_2O$) (Aldrich), sodium carbonate (Na_2CO_3) (Merck), 3-methylpyrozole-5-one (3MP5O) and nitric acid (HNO_3) 65% (Merck).

2.2. Preparation of nanosized $Ni_xMg_{1-x}Al_2O_4$ ceramic pigment

$Ni_xMg_{1-x}Al_2O_4$ pigments ($0.1 \leq x \leq 0.8$) were prepared by using metal chloride as a salt and then dissolved in distilled water, precipitated with sodium carbonate, good washing and drying. Then the above mixture was dissolved in nitric acid, heated to become clear solution, cooled to room temperature, and then 3-methylpyrozole-5-one (3MP5O) was added as a complexion agent. The resulting solution was heated until clear gel solution appears, transferred into furnace that was preheated to 450 °C. The precipitate initially started to swell and fill the beaker, producing a foamy precursor; this foam consists of very light and homogeneous flakes of very small particle size.
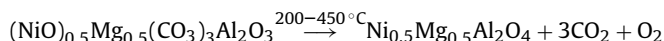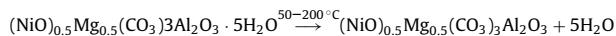
2.3. Characterization

Thermogravimetric analysis (TGA; DTA Instruments, SDT2960) of the precursor samples was studied using Shimadzu DT-50 thermal analyzer. Samples were carried out in static atmosphere of air against α-Al_2O_3 as a reference at a constant heating rate of 10 °C/min. The experiments were carried out in the temperature range between room temperature and 1000 °C. X-ray diffraction analysis was performed on SIEMENS D5000. The patterns were run with Cu-filtered Cu-Kα radiation (1.54 Å) energized at 45 kV and 10 mA. The samples were measured at room temperature in the range from $2\theta = (20–80°)$. Phase formation and particle size of product were identified by using X-ray diffraction analysis data. The morphology and particle shape for the calcinated powder were performed using TEM, modal EM 10 Zeiss, at 60 kV by dispersed sample in water on a copper grid. Infrared spectra of the samples were recorded in the range of 200–4000 cm^{-1} using Jasco FT/IR-460 plus. The method includes mixing few milligrams of calcinated powder of the sample with potassium bromide KBr powder in agate mortar. The mixture was then pressed by means of hydraulic press. The absorbance was automatically recorded against wave number cm^{-1}. The functional groups of calcinated powder were characterized by infrared spectra. The diffuse reflectance of fired pigments was measured in JASCO spectrophotometer UV–visible in 200–800 nm range using standard D65 illumination and barium sulfate as reference and the CIE-$L^*a^*b^*$ colorimetric method, recommended by the Commission International de l'Eclairage (CIE)

[36]. Spectrophotometer measurements were carried out using JASCO V530 UV/Vis Spectrophotometer in the range of 400–800 nm for both calcinated samples using 10 mm-matched quartz cells. The mixtures of prepared sample were calcinated in alumina crucibles.

3. Results and discussion

3.1. Thermal analysis

The thermogravimetric analysis for 0.50 mol of Ni^{2+} system using 3-methylpyrozole-5-one gives a weight losing of system changes in three steps as shown in TG-curve for ash material as present in Fig. 1. The loss of 18.5% (calc. 18.0%) by weight in the first step within the range 50–120 °C occurs by the elimination of the humidity water in sample. The lose of 38.5% (calc. 36.02%) in the second and third steps in the range 100–450 °C occurs due to evolution of $3CO_2$ and O_2 gases from sample. Four peaks in DTG curve that are shown at 80, 150, 280 and 450 °C. DTA shows four endothermic peaks at 80, 150, 250 and 700 °C and one exothermic peak at 450 °C. The first two endothermic peaks occur for the elimination of the water and the second for the decomposition of carbonate into CO_2. The exothermic peak is occurring due to complete combustion and elimination of the residual organic material in sample as carbon dioxide. The fourth endothermic peak is due to phase formation and appearance as horizontal line plateau assigned to formation of nano sized of suitable pure phase under this method. The calcination steps for this system can be represented as the following:

$$(NiO)_{0.5}Mg_{0.5}(CO_3)3Al_2O_3 \cdot 5H_2O \xrightarrow{50-200\,°C} (NiO)_{0.5}Mg_{0.5}(CO_3)_3Al_2O_3 + 5H_2O$$

$$(NiO)_{0.5}Mg_{0.5}(CO_3)_3Al_2O_3 \xrightarrow{200-450\,°C} Ni_{0.5}Mg_{0.5}Al_2O_4 + 3CO_2 + O_2$$

3.2. Infrared spectra

Infrared spectra (IR) for 0.10 (A), 0.50 (F), 0.80 (M) mol of Ni^{2+} systems using 3-methylpyrozole-5-one as fuel. IR curves demonstrated that the samples at ignition temperature 300 °C contain a broad absorption band around 3500 cm^{-1} for A system, 3490 cm^{-1} for F system and 3450 cm^{-1} for M system are related to the stretching vibration of free (–OH) group of water molecules. The absorption bands in range 1650–1050 cm^{-1} for A and F systems and 1630 cm^{-1} for M system are related to the stretching vibration of carbonyl (C=O and C–O) groups of residual organic fuel [37]. The absorption bands at 1650, 1450 and 858 cm^{-1} for A and F systems

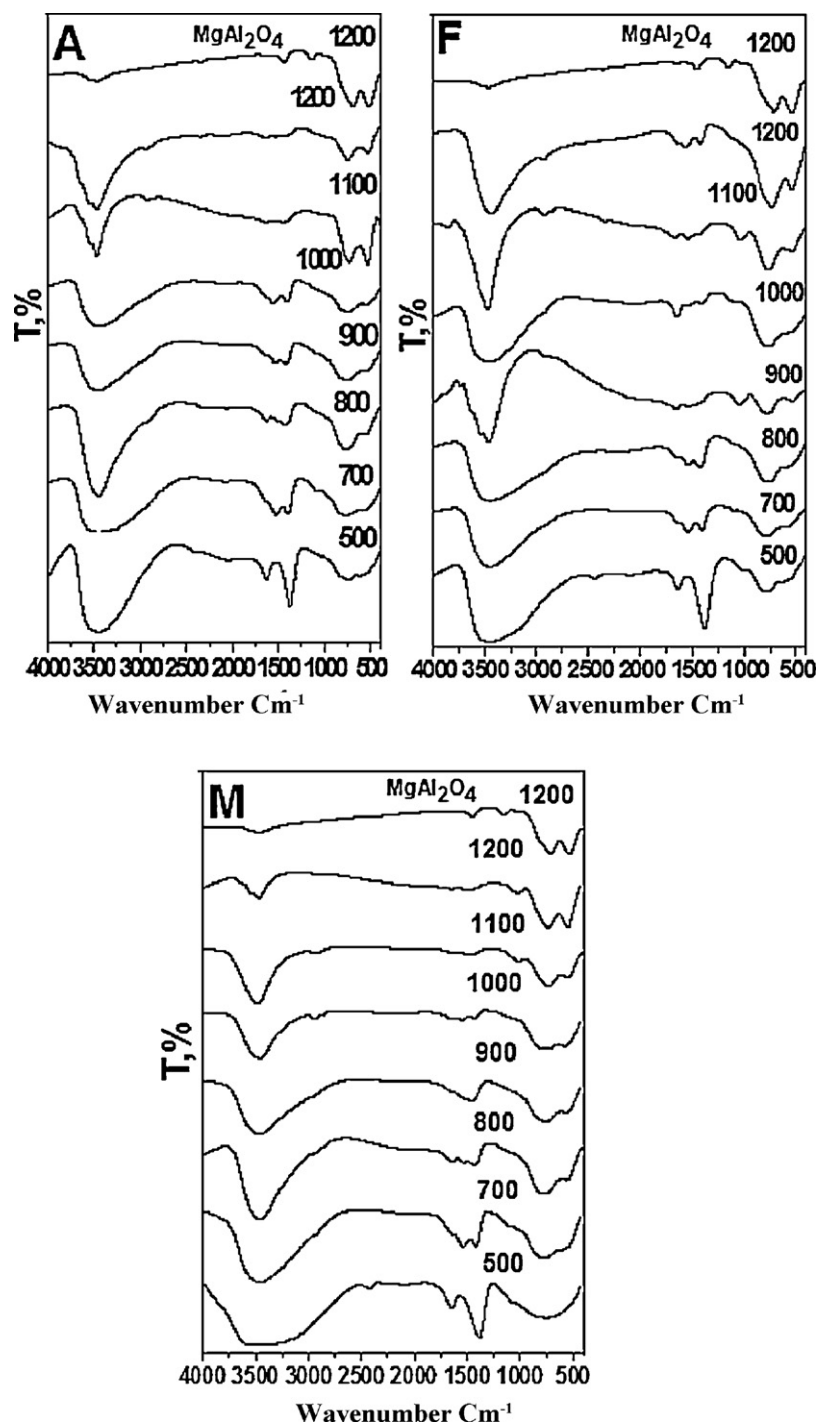**Fig. 2.** Infrared spectra for $Ni_{0.1}Mg_{0.9}Al_2O_4$ (A), $Ni_{0.5}Mg_{0.5}Al_2O_4$ (F) and $Ni_{0.8}Mg_{0.2}Al_2O_4$ (M) systems using 3-methyl pyrozole-5-one as fuel at different calcination temperatures.

and 1630, 1450 and 820 cm^{-1} for M system correspond to undecomposed nitrate ions. The absorption bands at 2950 for A and F systems and 2920 for M system related to C–H aliphatic in sample [38]. A weak absorption bands in range 400–700 cm^{-1} appear due to the formation of metal oxides. After calcinations at different temperatures from 500 to 1200 °C, the observed absorption bands in the range 800–4000 cm^{-1} are decreased gradually until disappeared at 1100 °C except, the strong absorption band at 3450 cm^{-1} for A and M systems and 3500 cm^{-1} for F system are related to the stretching vibration of adsorption water [39] molecules. The

three absorption bands 780, 740 and 530 cm^{-1} for A system and 770, 710 and 550 cm^{-1} for F and 760, 730 and 540 cm^{-1} for M systems are corresponding to AlO_4/AlO_6 groups building up the magnesium spinel as a result of vibration of ions of valence Al^{3+} in tetrahedral and octahedral positions compared with 700, 530 and 425 cm^{-1} for $MgAl_2O_4$ spinel. Other broad [40–42] bands at 700, 535 and 425 cm^{-1} for A system, 710, 550 and 425 cm^{-1} for F system and 760, 730 and 425 for M system are corresponding to NiO_6/NiO_4 and MgO_6/MgO_4 groups for the nickel and magnesium spinel as a result of vibration in the octahedral sites or to

Table 1
Assignment of the important bands in the IR spectra for 0.10, 0.50 and 0.80 mol of Ni^{2+} systems at different calcination temperatures using 3-methyl pyrozole-5-one as fuel.

Temperature (°C)	IR-band assignment						
	ν_{OH}	ν_{CH}	$\nu_{C=O}$	ν_{C-O}	ν_{C-N}	$\nu_{N=O}$	ν_{M-O}
0.10 mol of Ni^{2+}							
500	3400	2910	1650	1090	1382	800	700, 530
700	3450	2960	1650	–	1450	–	800, 500
800	3450	–	1650	–	1450	–	800, 520
900	3450	–	1650	–	–	–	740, 610, 530
1000	3450	–	–	–	–	–	740, 600, 530
1100	3450	–	–	–	–	–	760, 710, 620, 540, 425
1200	3500	–	–	–	–	–	760, 710, 620, 540, 425
0.50 mol of Ni^{2+}							
500	3450	2905	1637	1050	1450	800	760, 600
700	3450	2920	1650	–	1490	–	760, 520
800	3450	–	1650	–	1450	–	760, 530
900	3450	–	1650	–	–	–	760.530
1000	3450	–	–	–	–	–	770, 740, 660, 530
1100	3450	–	–	–	–	–	770, 740, 660, 535, 425
1200	3490	–	–	–	–	–	760, 720, 660, 535, 425
0.80 mol of Ni^{2+}							
500	3450	2980	1630	1050	1450	820	750
700	3400	2950	1650	1050	1450	810	760, 500
800	3450	–	1650	–	1450	–	760, 520
900	3450	–	1650	–	1450	–	760, 530
1000	3450	–	–	–	–	–	760, 530, 425
1100	3450	–	–	–	–	–	780, 730, 520, 425
1100	3450	–	–	–	–	–	780, 730, 530, 425
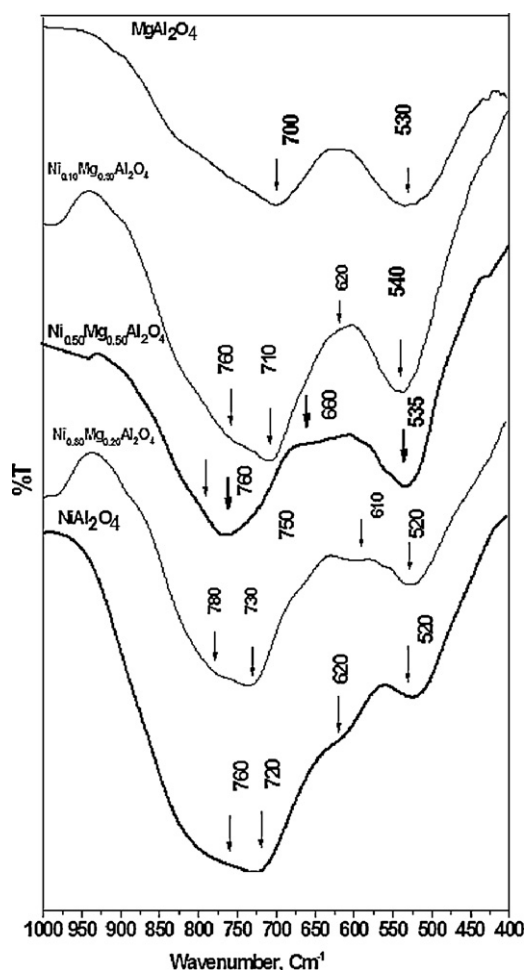
Fig. 3. Infrared spectra for 0.10, 0.50, 0.80 mol of Ni^{2+} systems, $NiAl_2O_4$ and $MgAl_2O_4$ by using 3-methyl pyrozole-5-one in range 400–1000 cm^{-1}.

mixed vibration of them in octahedral and tetrahedral sites [43,44] compared with 760–720–520 cm^{-1} for $NiAl_2O_4$ spinel as present in Figs. 2 and 3. The absorption band at 610 cm^{-1} characterizes for $NiAl_2O_4$ structure [45]. Assignment of important bands in the IR spectra for 0.10, 0.50 and 0.80 mol of Ni^{2+} systems at different calcination temperatures using 3-methylpyrozole-5-one as fuel is collected in Table 1.

3.3. Structure of nano ceramic pigments characterization

3.3.1. X-ray diffraction

Fig. 4 shows the X-ray diffraction (XRD) patterns of samples at different calcination temperatures. The prepared samples remained amorphous or contained only small crystallites lines with small amount of Al_2O_3 up to 700 °C. The effect of calcinations temperature on the growth of spinel phase of ceramic nano pigment powders begins to show the spinel crystalline with disappear Al_2O_3 phase in temperatures range 700–1200 °C [46,47]. The average crystallite sizes (*L*) are calculated from the X-ray diffraction peaks by using Scherrer equation [48];

$$\beta(2\theta) = \frac{0.9\lambda}{L\cos\theta}$$

where λ is the wavelength, θ is the diffraction angle and β is the corrected full width at half maximum of peaks. The crystalline spinel phase content and also the particles size increase with increasing calcination temperatures that are shown in Fig. 5. The density of 0.10, 0.50 and 0.80 mol of Ni^{2+} systems was calculated from X-ray and they are compared with experimental that obtained present in Table 2. The type of fuel is shown to directly effect on particles sizes of different systems of Ni^{2+} using 3-methylpyrozole-5-one calculated compared with the previous study [35], the XRD data are shown in Table 3.

3.3.2. Microstructure characterizations

Fig. 6 shows the photographs of powder samples under investigation and the spherical particles for 0.10, 0.50 and 0.80 mol of Ni^{2+} systems. The average particle size of pigment was measured
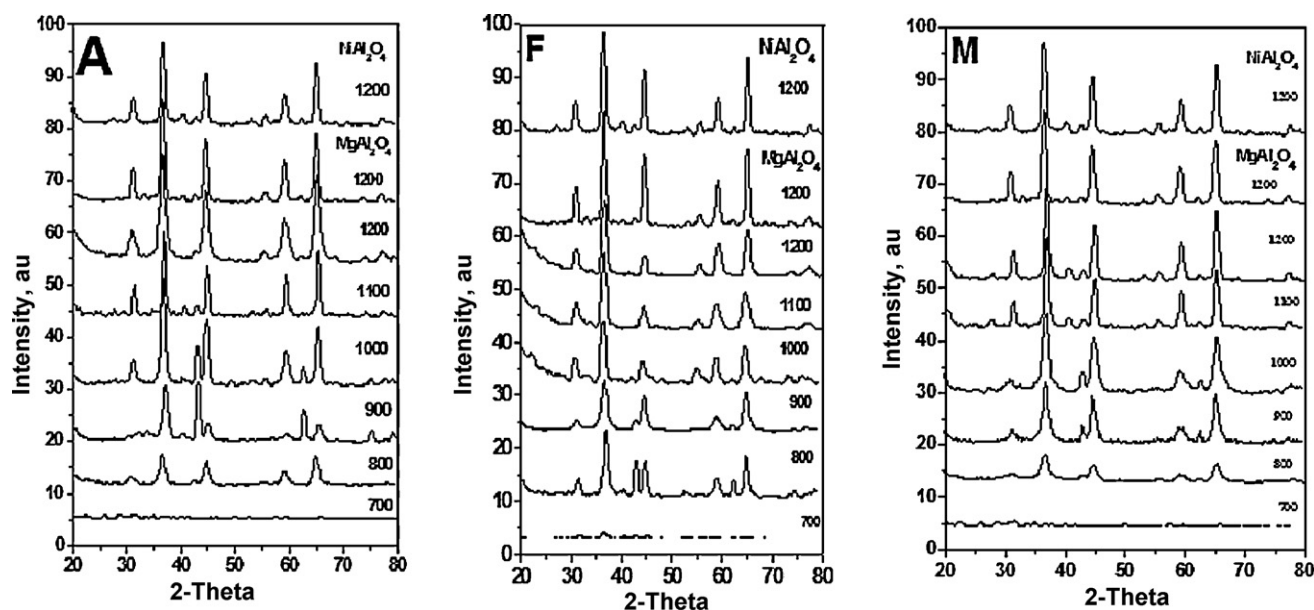
Fig. 4. X-ray diffraction for 0.10 (A), 0.50 (F) and 0.80 (M) mol of Ni^{2+} systems at different calcination temperatures using 3-methyl pyrozole-5-one as fuel.
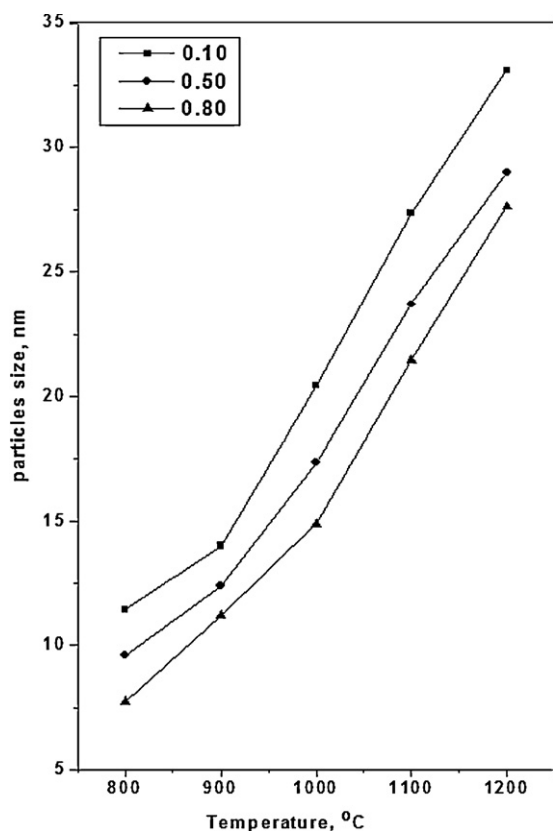

Fig. 5. The correlation between particle size from X-ray diffraction for A = 0.10, F = 0.50 and M = 0.80 mol of Ni^{2+} systems at different calcination temperatures using 3-methyl pyrozole-5-one.

by XRD and compared with the results were obtained from TEM as present in Table 4. The morphology and particle size decrease with increasing the amount of doping Ni^{2+} ion due to ionic radii decrease. The particle sizes are calculated using ultra structure size calculator or quantitative electron microscopy using a real analysis

using at least 20 particles that were required to characterize each size distribution from TEM photographs.

3.4. The characterization color of nano ceramic pigments

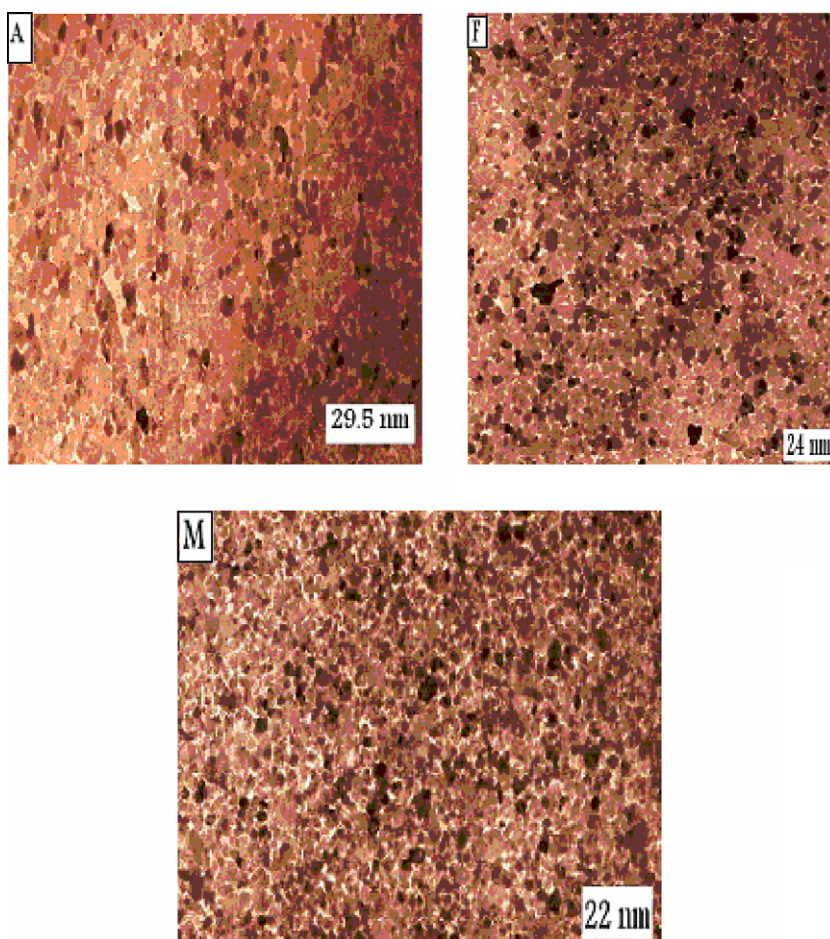#### 3.4.1. Diffuse reflectance spectroscopy (DRS)

Fig. 7 shows diffuse reflectance spectra (DRS) for 0.10, 0.50 and 0.80 mol of Ni^{2+} systems which represent as symbols A, F and M respectively. These systems show the appearance of band around 612, 500 and 460 nm for A system, 618, 500 and 445 nm for F system and 618, 500 and 450 nm for M system at 700 °C. These bands correspond to pale green-blue (cyan) color of sample under investigation. The bands shift to cyan band as calcination temperatures increase until reaching around 612, 570, 500, 505 and 460 nm for A system, 618, 560, 505 and 445 nm for F system and 618, 568, 505 and 450 nm for M system at 1000 °C for green-blue (cyan) color. The bands increase its shift to 460, 505 and 612 for A system, 445, 510 and 610 nm for F system and 450, 505, 560 and 606 nm for M system with increasing temperature up to 1200 °C [49,50] which show the good green-blue (cyan) color pigments. From colorimetric data present in Table 5, the values of b^* and a^* increase in the negative direction while L^* values decrease as result of increasing calcination temperatures. The increasing in negative values of a^* means the higher intensity of green color and the increasing values of b^* in negative direction indicate for the appearance of blue color as shown in Figs. 8 and 9. The increasing of a^* in negative direction is more than the increasing values of b^* in negative direction. This means the presence of two mixed colors green and blue such that the color intensity of green is more than the blue. The decrease in L^* parameter corresponds to reduction of the lightness of sample. The values of a^* and b^* increase in negative direction with the depth of green-blue color as result of calcination temperatures and the increasing of the amount of nickel ions. Colorimetric data show the high value of a^* and b^* and lower value of hue variation ΔE at 1200 °C for all doping nickel percents as shown in Table 5. This means that the appearance of good color of cyan ceramic pigment powders and a good color matching occurs at 1200 °C as shown in Fig. 10. The color of different doping with change temperature

Table 2
Lattice parameters and densities of different Ni^{2+} doping using 3-methyl pyrozole-5-one as fuel.

System	Lattice parameters	Calcinations temperature (°C)				
		800	900	1000	1100	1200
0.10	a	8.0806	8.085	8.0887	8.0948	8.1066
	a^3	527.63	528.49	529.22	530.42	532.75
	d_{theo} (g/ml)	3.662	3.656	3.651	3.643	3.628
	d_{exp} (g/ml)	3.653	3.650	3.645	3.637	3.620
0.50	a	8.070	8.075	8.085	8.0887	8.0948
	a^3	525.56	526.54	528.49	529.22	530.42
	d_{theo} (g/ml)	4.029	4.022	4.006	4.001	3.992
	d_{exp} (g/ml)	4.000	3.980	3.954	3.935	3.920
0.80	a	8.070	8.075	8.0806	8.085	8.0887
	a^3	525.56	526.54	527.63	528.49	529.22
	d_{theo} (g/ml)	4.292	4.284	4.276	4.269	4.262
	d_{exp} (g/ml)	4.266	4.253	4.245	4.233	4.215

a, lattice parameters; d_{theo}, theoretical density; d_{exp}, experimental density.

Table 3
Particle size (nm) from X-ray diffraction of different Ni^{2+} systems at different calcinations temperatures.

System	Calcination temperature (°C)						
	500	700	800	900	1000	1100	1200
0.1	Am^a	11.15	11.46	14.00	20.44	27.35	33.11
0.5	Am	10.65	9.60	12.40	17.35	23.69	29.00
0.8	Am	6.35	7.75	11.20	14.90	21.45	27.62

[a] Am, amorphous.

Fig. 6. TEM of A = 0.10, F = 0.50 and M = 0.80 of Ni^{2+} systems at 1100 °C temperature by using 3-methyl pyrozole-5-one.
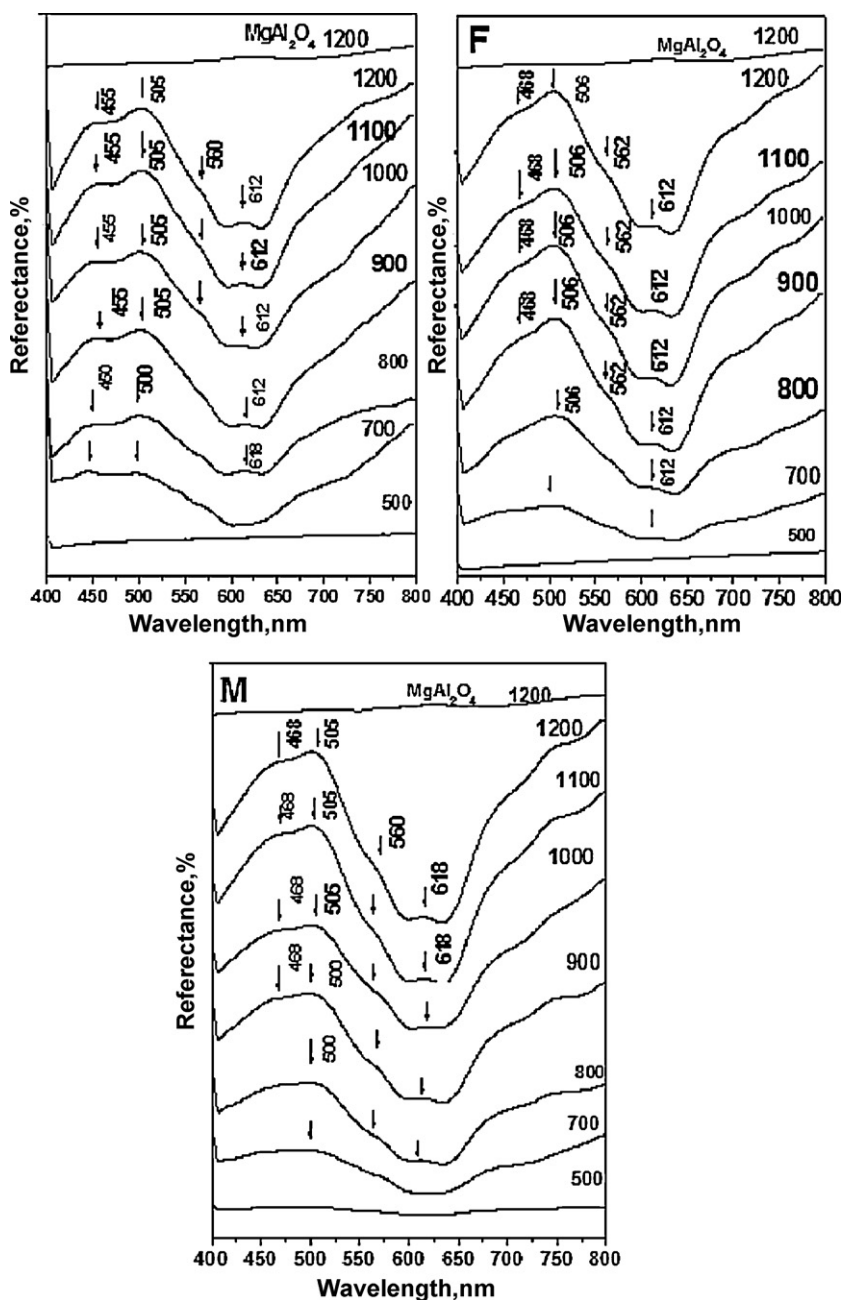
Fig. 7. The diffuse reflectance spectra for $Ni_{0.10}Mg_{0.90}Al_2O_4$ (A), $Ni_{0.50}Mg_{0.50}Al_2O_4$ (F) and $Ni_{0.80}Mg_{0.20}Al_2O_4$ (M) systems at different calcination temperatures by using 3-methyl pyrozole-5-one as fuel.

causes the lower value of hue variation ΔE that tends to a good color matching [51].

3.4.2. The electronic spectra of nano ceramic pigments

Fig. 11 shows the electronic spectra of nano ceramic pigments 0.10, 0.50 and 0.80 mol of Ni^{2+} ion systems using different calcination temperatures. Three broad absorption bands at 540 nm for A system, 560 nm for F system and 545 nm for M system (green region), 595 nm for A and F systems and 600 nm for M system (yellow-orange region) and 637 nm for A system, 535 nm for F and M systems (red region). These bands indicate for tetrahedral co-ordination for Ni^{2+} in the Al_2O_3 lattice which gives rise to the green-blue color. From Orgel diagram, the d–d transitions of Ni^{2+} ($3d^8_{Td}$) shows the presence of three transition states of

$^3T_{1g}(F) \rightarrow {}^1T_{2g}$, $^3T_{1g}(F) \rightarrow {}^3T_{1g}(P)$ and $^3T_{1g}(F) \rightarrow {}^3A_{2g}$. The two weak absorption bands at 475, 480 nm and 725, 715 nm indicate for octahedral co-ordination of Ni^{2+} in the Al_2O_3 lattice [52,53] and the energy level diagram gives d-d transitions of Ni(II) ($3d^8_{Oh}$) from Orgel diagram that shows $^3A_{2g} \rightarrow {}^3T_2(D)$, $^3A_{2g} \rightarrow {}^3T_1(F)$. This triple

**Table 4**
XRD and TEM average particle sizes (nm) data of different Ni^{2+} systems at 1100 °C.

System	Average particle sizes (mm)	
	XRD	TEM
0.10	27.35	29.50
0.50	23.69	24.28
0.80	21.45	22.35

Table 5
Colorimetric data for 0.10, 0.50 and 0.80 mol of Ni^{2+} systems at different calcination temperatures using 3-methyl pyrozole-5-one as fuel.

System	Temperature	L^*	a^*	b^*	ΔE
0.10	500	96.94	1.02	0.06	96.95
	700	95.17	−1.34	−1.11	95.19
	800	94.4	−1.65	−1.49	94.43
	900	93.89	−1.88	−1.53	93.92
	1000	91.98	−2.18	−1.65	92.02
	1100	91.56	−2.47	−1.85	91.61
	1200	90.00	−5.25	−2.59	90.19
0.50	500	89.21	0.81	3.71	89.29
	700	92.97	−2.51	−130	93.00
	800	91.79	3.61	−0.64	91.90
	900	89.28	−4.27	−1.18	89.39
	1000	86.34	−4.46	−1.19	86.46
	1100	85.92	−7.58	−3.00	86.31
	1200	85.93	−8.17	−3.43	86.39
0.80	500	81.13	1.83	3.29	81.22
	700	94.84	−2.01	−233	94.89
	800	93.41	−3.44	−3.11	93.53
	900	91.66	−5.42	−4.22	91.92
	1000	88.91	−6.94	−4.18	89.28
	1100	88.60	−9.96	−5.77	89.35
	1200	84.18	−14.48	−7.85	85.78
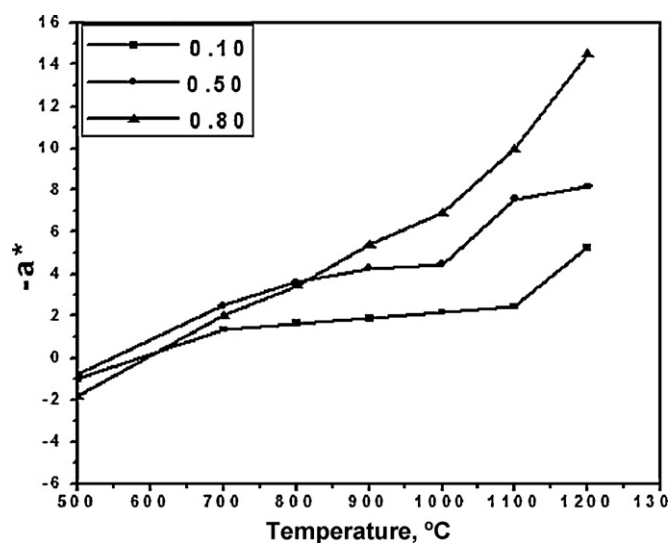
Fig. 8. The correlation between a^* and calcination temperature for 0.10, 0.50 and 0.80 mol of Ni^{2+} systems by using 3-methyl pyrozole-5-one as fuel.
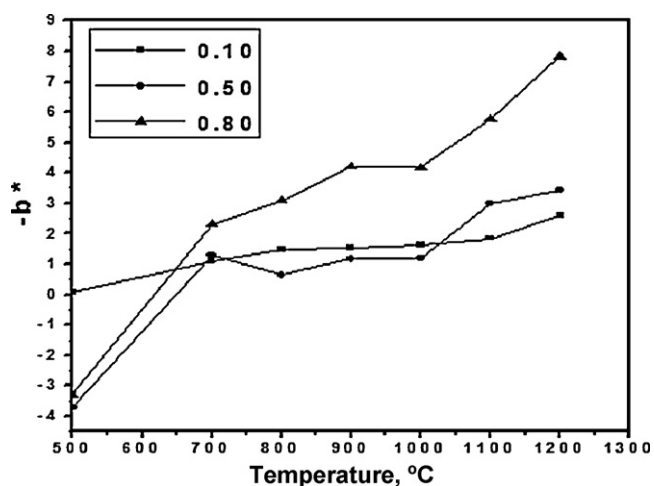
Fig. 9. The correlation between b^* and calcination temperature for 0.10, 0.50 and 0.80 mol of Ni^{2+} systems by using 3-methyl pyrozole-5-one as fuel.

Fig. 10. The color of ceramic powder for 0.10, 0.50 and 0.80 mol of Ni^{2+} systems using 3-methyl pyrozole-5-one as a fuel at different calcination temperature.
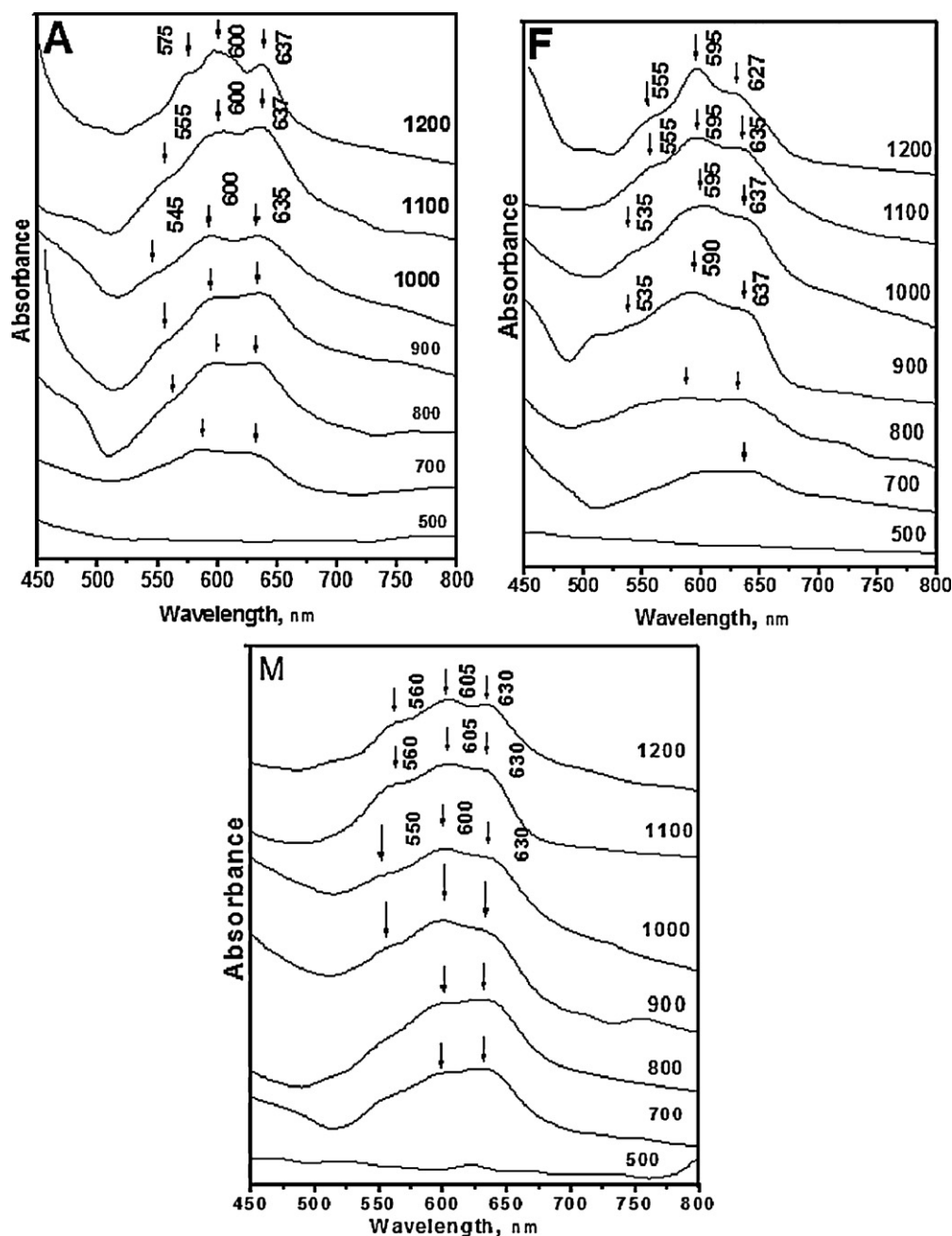
Fig. 11. The electronic spectra for $Ni_{0.10}Mg_{0.90}Al_2O_4$ (A), $Ni_{0.50}Mg_{0.50}Al_2O_4$ (F) and $Ni_{0.80}Mg_{0.20}Al_2O_4$ (M) systems at different calcination temperature by using 3-methyl pyrozole-5-one as fuel.

band in visible region can be attributed to Jahn–Teller [54,55] distortion of octahedral structure.

4. Conclusions

$Ni_xMg_{1-x}Al_2O_4$ ($0.1 \leq x \leq 0.8$) as cyan coloring agent of ceramic pigments has been successively prepared by using low temperature combustion reaction (LTCR) method and 3-methylpyrozole-5-one as fuel. Characterization of nano refractory pigments is studied by infrared spectroscopy (IR), electronic spectroscopy, diffuse reflectance spectroscopy (DRS), thermal analysis techniques, X-ray diffractions (XRD) and transmission electron microscopy (TEM). The calcination temperatures in range 500–1200 °C give nanosized oxides with particle sizes in the range of 6.35–33.11 nm. The particle sizes increased as sintering of samples at different calcinations temperatures and TEM shows spherical shape with nano-scale up to 1200 °C. FT-IR and XRD show the formation of single spinel structure at 700 °C. Cyan color intensity increased as the amount of nickel ion increased and calcination temperatures and time. Also, the visible spectra give broad absorption band with triple heads as result of Jahn–Teller distortion of octahedral structure.

References

[1] M. Cain, R. Morrell, Appl. Organomet. Chem. 15 (2001) 321.
[2] Z. Hu, M. Xue, Q. Zhang, Q. Sheng, Y. Liu, Dyes Pigm. 76 (2008) 173.
[3] F.J. Maile, G. Pfaff, P. Reynders, Prog. Org. Coat. 54 (2005) 150.
[4] H.M. Smith, High Performance Pigments , Wiley-VCH Verlag, Weinheim, 2002.
[5] S.K. Biswas, D. Dhak, A. Pathok, P. Pramanik, Mater. Res. Bull. 43 (2008) 665.
[6] E.Sh. Kharashvili, Glass Ceram. 42 (1985) 459.
[7] R.W. Batchelor, Trans. Br. Ceram. Soc. 73 (1974) 297.
[8] B. Yang, J.M. Huang, E.C. Hao, Chem. J. Chin. Univ. 18 (1997) 1219.

[9] I.H. Gul, A. Maqsood, M. Naeem, M.N. Ashiq, J. Alloys Compd. 507 (2010) 201.
[10] W.S. Cho, M. Kakihana, J. Alloys Compd. 287 (1999) 87.
[11] T. Mimani, J. Alloys Compd. 315 (2001) 123.
[12] L. Gama, M.A. Ribeiro, B.S. Barros, R.H.A. Kiminami, I.T. Weber, A.C.F.M. Costa, J. Alloys Compd. 483 (2009) 453.
[13] J. Livage, Sol–gel synthesis of inorganic materials , in: Encyclopedia of Materials: Science and Technology, 2008, pp. 4105–4108.
[14] D. Segal, J. Mater. Chem. 7 (8) (1997) 1297.
[15] C.O. Arean, M.P. Mentruit, E. Escalona, F.X. llablresi Xamena, J.B. Parra, Mater. Lett. 12 (1999) 537.
[16] P.P. Phule, T.E. Wood, Sol–gel synthesis of ceramics and glasses , in: Encyclopedia of Materials: Science and Technology, 2008, pp. 1090–1095.
[17] M. lade, H. Mays, J. Schmidt, R. Willumeit, R. Schomacker, Colloids Surf. A: Phys. Chem. 163 (2000) 3.
[18] R.E. Riman, W.L. Suchanek, M.M. Lencka, Ann. Chim. Sci. Mater. 27 (2002) 15.
[19] Z. Chen, E. Shi, W. Li, Y. Zheng, N. Wu, W. Zhong, J. Am. Ceram. Soc. 85 (2002) 2949.
[20] Y.W. Chen, T.M. Yen, C. Li, J. Non-Cryst. Solids 185 (1995) 49.
[21] J.R. Osman, J.A. Crayston, A. Pratt, D.T. Richens, Mater. Chem. Phys. 110 (2008) 256.
[22] K.T. Kim, C. Kim, J. Eur. Ceram. Soc. 24 (2004) 2613.
[23] M. Kakihana, J. Sol-Gel Sci. Technol. 6 (1996) 7.
[24] X. Yu, X. He, S. Yang, X. Yang, X. Xu, J. Mater. Lett. 58 (2003) 48.
[25] R. Ianos, I. Lazau, C. Pǎcurariu, P. Barvinschi, Mater. Res. Bull. 43 (2008) 3408.
[26] X.H. Huang, J. Chang, Mater. Chem. Phys. 115 (2009) 1.
[27] M.D. Nersesyan, A.G. Peresada, A.G. Merzhanov, Int. J. SHS 7 (1998) 60.
[28] J. Calbo, M.A. Tena, G. Monros, M. Llusar, J.A. Badenes, J. Sol-Gel Sci. Technol. 38 (2006) 167.
[29] M. Martosa, B. Julian, H. Dehouli, D. Gourier, E. Cordoncillo, P. Escribano, J. Solid State Chem. 180 (2007) 679.
[30] M. Trojan, P. Siulcova, P. Mosiner, Dyes Pigm. 44 (2000) 161.
[31] A.L.M. de Oliveira, J.M. Ferreira, M.R.S. Silva, G.S. Braga, L.E.B. Soledade, M.A.M. Maria Aldeiza, A.P. Carlos, S.J.G. Lima, E. Longo, A.G. de Souza, I.M. Garcia dos Santos, Dyes Pigm. 77 (2008) 210.
[32] Ekambaram, J. Alloys Compd. 390 (2005) 14.
[33] I.S. Ahmed, H.A. Dessouki, A.A. Ali, Spectrochim. Acta A 71 (2008) 616.
[34] I.S. Ahmed, S.A. Shama, M.M. Moustafa, H.A. Dessouki, A.A. Ali, Spectrochim. Acta A 74 (2009) 665.
[35] I.S. Ahmed, H.A. Dessouki, A.A. Ali, Polyhedron 30 (2011) 584.
[36] CIE, Recommendations of Uniform Color Spaces, Color Difference Equations, Psychometrics Color Terms, Supplement No. 2 of CIE Publ. No. 15 (E1-1.31), 1971, Bureau Central de la CIE, Paris, 1978.
[37] P. Duran, J. Tartaj, F. Rubio, C. Moure, O. Pena, J. Ceram. Int. 31 (2005) 599.
[38] A.K. Adak, A. Pathak, P. Ramanik, Brit. Ceram. Trans. 98 (1999) 200.
[39] M.F.M. Zawrah, A.A. El Kheshen, Brit. Ceram. Trans. 101 (2002) 71.
[40] A.Yu. Chapskaya, N.I. Radishevskaya, N.G. Kasatskii, O.K. Lepakova, Yu.S. Naiborodenko, V.V. Vereshchagin, Glass Ceram. 62 (2005) 11.
[41] L.F. Koroleva (Chekhomova), Glass Ceram. 61 (2004) 9.
[42] N.N. Boguslavska, E.F. Venger, N.M. Vernidub, Yu.A. Pasechnik, K.V. Shportko, Semicond. Phys. Quant. Electron. Optoelectron. 5 (1) (2002) 95.
[43] C. Wang, S. Liu, L. Liu, X. Bai, J. Mater. Chem. Phys. 96 (2006) 361.
[44] K. Nakamoto, Infrared and Raman Spectra of Inorganic and Coordination Compounds , fourth ed., Wiley Press, New York, 1986, p. 231.
[45] N. Thanabodeekij, M. Sathupunya, A.M. Jamieson, S. Wongkasemjit, Mater. Charact. 50 (2003) 325.
[46] Y.S. Han, J.B. Li, X.S. Ning, X.Z. Yang, B. Chi, Mater. Sci. Eng. A 369 (2004) 241.
[47] O. Quhard, Ch. Laurent, M. Brieu, A. Rousset, Nanostruct. Mater. 7 (1996) 497.
[48] P. Klug, L.E. Alexander, X-ray Diffraction Procedure for Polycrystalline and Amorphous Materials , Wiley, New York, 1974, p. 634.
[49] M. Jitianu, A. Jitianu, M. Zaharescu, D. Crisan, R. Marchidan, Vib. Spectrosc. 22 (2000) 75.
[50] M. Jitianu, M. Balasoiu, R. Marchidan, M. Zaharescu, D. Crisan, M. Craiu, Int. J. Inorg. Mater. 2 (2000) 287.
[51] F. Bondioli, T. Manfredini, M. Romagnoli, J. Eur. Ceram. Soc. 26 (2006) 311.
[52] P. Jeevanandam, Yu. Koltypin, A. Gedanken, Mater. Sci. Eng. B 90 (2002) 125.
[53] C.F. Song, M.K. Lu, F. Gu, S.W. Liu, S.F. Wang, D. Xu, D.R. Yuan, Inorg. Chem. Commun. 6 (2003) 523.
[54] C.R. Bambord, Phys. Chem. Glasses 3 (1962) 189.
[55] T. Bates, Ligand field theory and absorption spectra of transition-metal ions in glasses , in: Modern Aspects of the Vitreous State, vol. 2, Butterworths, London, 1961, pp. 195–254.